Surface acoustic waves in Ni/V superlattices

R. Danner and R. P. Huebener
Physikalisches Institut II, Universität Tübingen, D-7400 Tübingen, Federal Republic of Germany

C. S. L. Chun, M. Grimsditch, and Ivan K. Schuller
Materials Science and Technology Division, Argonne National Laboratory, Argonne, Illinois 60439
(Received 7 October 1985)

We have measured the surface-acoustic-wave velocities in Ni/V superlattices using both Brillouin scattering and surface-acoustic-wave techniques; the results are in good quantitative agreement. These results confirm earlier reports of phonon-velocity softening in bcc/fcc superlattices and prove that this is a general phenomenon, not a consequence of the measurement method. In addition, we describe in detail the ultrasonic measurement technique which allowed measurements to be performed in thin films.

I. INTRODUCTION

Since the early stages of development in the field of metallic superlattices, considerable effort has been invested in determining their elastic constants.[1] Much of the excitement was motivated by the original reports of large enhancements of the biaxial modulus of the superlattices (Cu/Ni) that form solid solutions in their binary phase diagram.[2] These early results have been confirmed by independent measurements of the Young and torsional modulii.[3] Some criticisms have also been raised about these measurements[4,5] and so far no theoretical model has been advanced that can explain these anomalous enhancements ("supermodulus effect") in a *quantitative* fashion.[6] Superlattices whose constituents *do not* form solid solutions in their binary phase diagram (i.e., Nb/Cu,Mo/Ni) have received more recent attention.[7,8] The elastic shear modulus has been measured using Brillouin scattering techniques, and observations of a softening ($\sim 35\%$) of this modulus have been reported. The advantage of Brillouin scattering over mechanical measurements is that the superlattice can be measured directly without removal from the substrates. A drawback of Brillouin scattering is that extremely good surface quality is required. These measurements have been found to be correlated with a metal-nonmetal transition in the electrical resistivity and an average lattice expansion ($\sim 2\%$) perpendicular to the layers.[8] Although the theoretical reasons for these anomalies are not completely settled, a theoretical calculation has been presented[9] which explains *quantitatively* the softening as being due to the observed lattice expansion.

Because superlattices are prepared in the form of thin films, conventional ultrasonic techniques are not easily applicable. Here we report what we believe is the first ultrasonic study of surface acoustic waves (SAW) in superlattices. This technique is nondestructive and it can be compared directly with Brillouin scattering results since the same elastic constant is measured. In order to avoid any doubt about these comparisons, Brillouin scattering experiments were performed prior to SAW measurements on the same samples.

II. SAMPLE PREPARATION AND CHARACTERIZATION

The samples (~ 1.5–$2\ \mu$m thick) were prepared using a sputtering technique developed earlier.[10] The substrates (optically polished $LiNbO_3$, Al_2O_3, and freshly cleaved mica) were held onto a temperature-controlled, rotating sample holder. Two beams of sputtered particles were prepared using high-rate magnetron sputtering. The rates were controlled by stabilizing the power into the sputtering guns and the substrates were held sufficiently far from the sputtering gun to avoid interaction with the plasma and to allow the sputtered species to thermalize in the inert Ar gas.

Extensive x-ray characterization has been performed using high- and low-angle x-ray diffraction techniques.[11] The details of these studies will be the subject of a future publication.[12] The structure is found to be quite similar to the earlier studied Nb/Cu (Ref. 11) and Mo/Ni (Ref. 8) superlattices. Briefly, the samples consist of crystalline, well-segregated Ni(111) and V(110) layers with a perpendicular coherence length of ~ 1000 Å and an in-plane grain size of ~ 50 Å. In the plane the sample is polycrystalline although the layers extend over a large area, as indicated by the small-angle x-ray diffraction.

The contamination of the layer is found to be below the detection limit in ion mill Auger experiments beyond about 50–100 Å from the surface. The lack of oxygen and carbon contamination is also indicated by the fact that the superconducting transition temperature of thick V superlattices is close to that of bulk V.[13]

III. BRILLOUIN SCATTERING

Brillouin scattering measurements were performed on the samples deposited on $LiNbO_3$ substrates for SAW measurements. The measurements were performed at room temperature using a five-pass Fabry-Perot interferometer. About 150 mW of single-moded radiation ($\lambda \sim 5145$ Å) polarized in the scattering plane, from an Ar^+ laser were incident on the sample. No analyzer was used in the scattered beam. The frequency shifts were

at least three points on the dispersion curve, and the velocity of the surface wave was determined from the slope of the dispersion curve. Since the samples are much thicker than the phonon wavelength under study ($\sim$4000 Å), no corrections due to the substrate are necessary. The errors were estimated based on the reproducibility of the measurements. The variations from sample to sample were slightly greater than variations from place to place on the same sample which in turn were larger than the variations obtained at the same spot while changing the wave vector. We note that no *systematic* difference was found between samples deposited on mica and $LiNbO_3$. The measurements reported here are the ones performed on the $LiNbO_3$ substrates.

IV. ULTRASONIC MEASUREMENTS

Since this type of measurement is applied for the first time to superlattices and since the accuracy required is higher in this case than ordinarily, we shall describe it in detail. SAW waves were generated by standard piezoelectric techniques on optically polished $LiNbO_3$ substrates. The $LiNbO_3$ substrates, cut in the *YZ* orientation, were 1 mm thick and had a rectangular shape with a 10×20-mm area.

Prior to the fabrication of the Ni/V superlattice films described in Sec. II, interdigital transducers were attached to the surface of the $LiNbO_3$ substrates, serving in the usual way as generators and detectors for the SAW. Niobium film (2000 Å thick) transducers were prepared by rf sputter deposition and standard photolithographic techniques. The geometrical arrangement of the interdigital transducers is shown schematically in Fig. 1. Each $LiNbO_3$ substrate carried four transducers, two of which were to be used as generators and two as detectors. The superlattice film to be investigated was placed between one generator-detector pair, whereas the surface between the other pair was kept free. In this way each substrate carried also a reference path, allowing a highly accurate comparison of the velocity data for the different superlattice films prepared on different substrates.

Each transducer contained a total of 50 digits, each 5 μm wide. The width of the opening between two neighboring digits was also 5 μm. Hence, the acoustic wavelength was 20 μm and the optimum operation frequency of the transducers was 176 MHz. The aperture of the transducers was 0.5 mm and the inner distance between generator and detector was close to 1.5 cm. By careful alignment of the photolithography projection mask, the path-length difference between the two generator-detector pairs on each substrate could be kept below 20 μm, i.e., below the acoustic wavelength. This was checked using a measuring microscope and also by measuring the traveling time of a pulsed SAW between both generator-detector pairs for each substrate, *prior to the fabrication of the superlattice films.* The exact path length between both generator-detector pairs on each substrate was determined by comparing the phase of both detector signals interferometrically using a vector voltmeter. In this way the traveling time of the SAW for both paths on each substrate could be measured with an accuracy of about 15 ps, corresponding to an accuracy for the path lengths of about 0.1 μm, or $\sim$2 ppm. These control measurements were performed prior to the fabrication of the superlattice films. During these controls the ultrasonic measuring principles used were identical to those described below for the completed samples. All subsequent data obtained for the completed samples were corrected for any small path-length difference found during these control measurements.

The superlattice films (4.5 mm wide, $\sim$12 mm long) were placed nearly symmetrically between the corresponding generator-detector pair. Since the superlattice film was much wider than the aperture of the transducers, it did not act as a wave guide and the excitation of other vibrational modes in addition to the Rayleigh wave could be avoided. The area of the superlattice film was defined by means of a mechanical mask placed close to, but not in contact with, the substrate surface during the fabrication of the superlattice. Because of the small distance between mask and substrate and the consequent smearing of the edges of the film, appreciable reflections of the SAW at the film boundaries could be avoided. Since SAW's are emitted by the generator in both directions, it is important to eliminate the acoustic wave emitted backwards and reflected at the end of the $LiNbO_3$ substrate. This was accomplished by roughening the corresponding substrate edge and by covering it with vacuum grease.

To detect the small differences in the velocity of the SAW's for the different superlattice films, we have modified the twin-specimen interferometer principle[14] and combined it with the time-marker principle.[14] In this way it has been possible to measure small velocity *changes* cor-

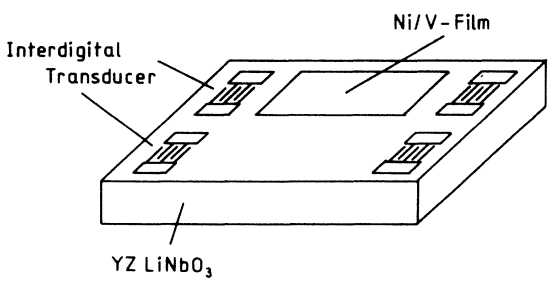

FIG. 1. Geometrical arrangement of transducers and superlattice on the $LiNbO_3$ substrate.

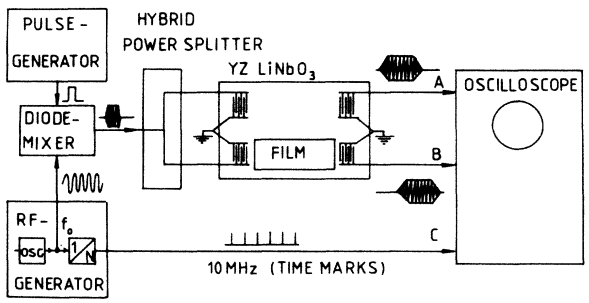

FIG. 2. Block diagram of electronics for the SAW measurement.

responding to an accuracy of 5 ppm, even though the *absolute* phase velocity could be obtained only with 0.01% accuracy. Using the uncovered reference path for a difference measurement, the influence of the individual substrates and of small temperature variations between measurements for the different samples could be eliminated.

The velocity of the SAW's was measured using a pulse technique. The electronic arrangement is shown schematically in Fig. 2. A pulse generator producing rectangular pulses (0.5 μs wide) with a rise time less than 5 ns served for turning a 176-MHz high-frequency signal periodically (20-kHz repetition rate) on and off via a diode mixer. The 176-MHz signal was obtained from a quartz-stabilized frequency generator. Using a hybrid power splitter, the pulsed high-frequency voltage was split into two phase-coherent signals of equal magnitude which were fed to the two input transducers. An additional matching element

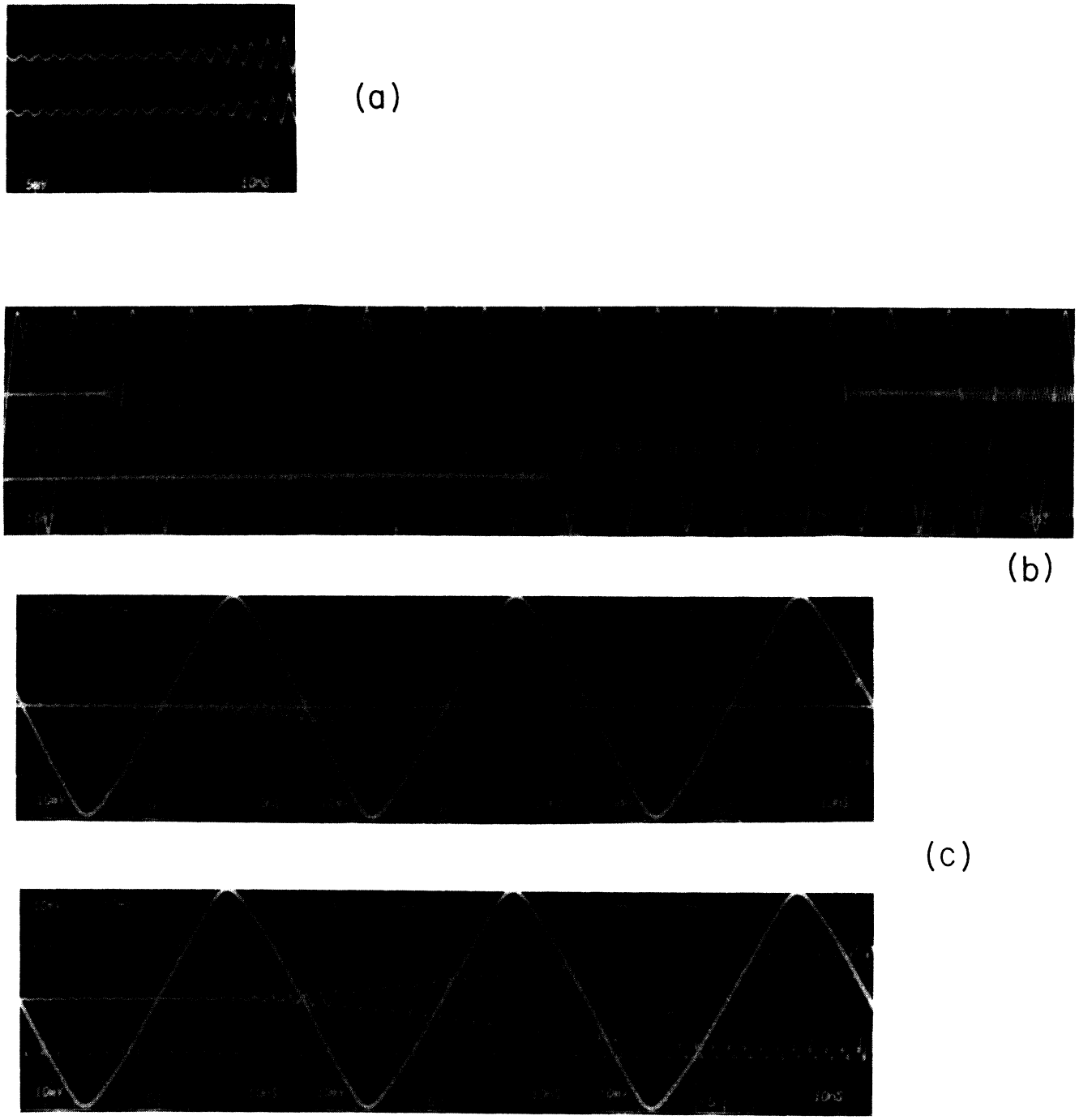

FIG. 3. Oscilloscope traces obtained as described in the text.

served for compensating any impedance mismatch between both input transducers.

The reference output signal (channel A) and the sample output signal (channel B) are synchronously displayed using a multichannel oscilloscope (Tektronix model 7904). To obtain sufficient time resolution, the oscilloscope was operated using a dual time base (500 ps/division, Tektronix model 7B92A). In this way a time-delayed display on the oscilloscope with high time resolution was possible. However, at this high time resolution the onset of the two pulses from both channels could not be displayed on the oscilloscope simultaneously.

In order to measure appreciable time delays between both pulses with high time resolution, a time marker at a repetition rate of 10 MHz was also displayed on the oscilloscope using the third channel C. This time-marker signal was supplied directly from an internal testpoint of the oscillator and was phase coherent with the 176-MHz signal. In this way a jitter-free display on the oscilloscope could be obtained. The 10-MHz time markers allowed a visual control of the time period selected for display and of its location on the time axis with high time resolution.

For an accurate time-of-flight measurement, the delayed pulse signals for the reference path (channel A) and for the sample path (channel B) were photographed from the oscilloscope. As an example, we show in Fig. 3(a) the signals of channels A and B of the sample before the $\Lambda = 36.2$ Å Ni/V superlattice film was prepared. Figure 3(b) shows the signals in both channels after the preparation of the Ni/V superlattice film for the same sample. In Fig. 3(c) we present again the signals in both channels after the preparation of the Ni/V superlattice film, on an expanded time scale. Figures 3(b) and 3(c) are compositions of a sequential series of individual photographs obtained for various corresponding time shifts for the oscilloscope display. All ultrasonic measurements described in this article were performed at room temperature.

By counting the 10-MHz time markers, the approximate time position (on a 0.1-μs scale) of the output pulses was obtained. Subsequently, the time position was found with high time resolution by relating the onset of the output pulses to the corresponding steep rising slope of the phase-coherent 10-MHz signal. Here the accurate position of the onset of the output pulses was obtained by linear extrapolation of the rising part of the 176-MHz pulse [see Fig. 3(c)] to zero amplitude. In this way the onset of the output pulses could be determined within an accuracy of about 200 ps. Following this approximate measurement of the time delay between channels A and B, the temporal phase difference between both channels was determined with higher accuracy interferometrically using a vector voltmeter (Rohde and Schwarz model ZPV1). In this way the relative shift in phase between both channels could be found with an uncertainty of about 20 ps. As mentioned above, the measured difference between the delay times of channels A and B were corrected for any small difference in path length of the two channels detected ultrasonically prior to the fabrication of the superlattice films.

Finally, the phase velocity v of the SAW in the Ni/V-$LiNbO_3$ system was obtained from the expression

$$v = \left[\frac{1}{v_0} + \frac{\Delta t}{L} \right]^{-1} . \tag{1}$$

Here, v_0 is the phase velocity in the uncovered $LiNbO_3$ substrate, Δt the corrected delay between channels A and B, and L the length of the superlattice film. The overall accuracy of the phase velocity v was limited by the uncertainty in the length L. Due to the sloping edges of the superlattice films (which were necessary for minimizing reflections of the SAW), the length L could be determined only within an accuracy of 10 μm using a measuring microscope. For v_0 we have taken the value $v_0 = 3488$ m/s.[15]

V. EXPERIMENTAL RESULTS

The ultrasonic measurements described in Sec. IV yield the phase velocity of the SAW's for the *combination* of the Ni/V superlattice films and the $LiNbO_3$ substrates. The penetration depth of the Rayleigh waves is about one wavelength, i.e., in our case about 20 μm. On the other hand, the thickness of the superlattice films is only about 1.5–2 μm. Hence, the propagation of the SAW's is determined not only by the superlattice films but also by the underlying $LiNbO_3$ substrate.

The original velocity data for the different samples, calculated from the measured time delay Δt using Eq. (1), are listed in Table I. To obtain the elastic properties of the pure superlattice films without the influence of the substrate, the original data were treated further using the following considerations. As a starting point we must look for a systematic dependence of the phase velocity upon the thickness of the superlattice film on the $LiNbO_3$ substrate. Here we treat the superlattice films as a homogeneous medium, since the modulation length in the superlattice films is much smaller than the wavelength of the SAW. To obtain the exact dependence upon the film thickness, the acoustic-wave equations must be solved with the correct boundary conditions.[16,17] Even in the simplest cases this requires extensive numerical analysis which, given the uncertainty in film thickness, is not warranted. As a simpler alternative, it has been proposed to expand the phase velocity in a power series of the normalized film thickness.[18,19] In our case, such an approach was impossible, since only a single value of the phase velocity was experimentally available for a specific total thickness of the superlattice film and a specific modulation wavelength. Because of these difficulties we have approximated the dependence of the phase velocity on the normalized film thickness by a simple analytic function.

For the two components of our superlattice films, nickel and vanadium, the transverse and longitudinal sound velocities are smaller than those in the YZ $LiNbO_3$ substrate. Hence, the phase velocity decreases with increasing film thickness. (In our case we can restrict ourselves only to the first Rayleigh mode in view of the total thickness of our films.) We approximate the dependence of the phase velocity v on the normalized film thickness kh by the function

$$v(kh) = v(\infty) + [v(LiNbO_3) - v(\infty)][1 - \tanh(kh)] . \tag{2}$$

TABLE I. Sample characteristics and results.

Modulation wavelength (Å)	h (μm) x-ray	h (μm) Dektak[a]	h (μm) Interferometer	L (mm)	$v(kh)$ (m/s)
36.2	1.816		1.603	12.56	2909
16.4	1.638	1.563	1.444	12.65	2907
13.9		1.200	1.142	12.49	3044
81.8	1.903	1.875	1.886	12.37	2896
Nifilm		0.440	0.470	12.34	3208
Vfilm		1.788	1.785	12.43	3034
930.0		1.909	2.002	12.59	2882
50.8	1.725	1.607	1.642	12.38	2911
18.5	1.853	1.764	1.708	12.35	2857
138.7	1.990	1.884	1.833	12.38	2938
633.0	1.425	1.425	1.480	12.34	3004

[a]Sloan Technical Corporation, 535 East Montecito Street, Santa Barbara, CA 93103.

Here, k is the wave vector of the SAW, h the thickness of the superlattice film, and $v(\infty)$ and $v(LiNbO_3)$ are the phase velocities for an infinite thickness superlattice film and for the $LiNbO_3$ substrate, respectively. Using expression (2) we can calculate the quantity $v(\infty)$ we are looking for from the two values $v(kh)$ and $v(LiNbO_3)$ given experimentally. The phase velocity $v(\infty)$ obtained in this way is plotted in Fig. 4 (dots) versus the modulation wavelength. In order to check this procedure for finding $v(\infty)$, we have compared this method with numerical results available in the literature[17,20–22] and have found excellent agreement.

As mentioned earlier, the Brillouin scattering measurements only probe a depth of about 4000 Å from the film surface. Because of this and the experimental accuracy, it is not necessary to correct for substrate effects.

Figure 4 shows the $v(\infty)$ measurements (dots) together with the velocities determined from Brillouin scattering measurements (crosses). Both measurements are found to be in reasonably good agreement, showing the existence of the softening at low superlattice thicknesses quite clearly. This agreement is also an indication that the analysis described earlier to extract $v(\infty)$ from the measurements is correct. At this point it should be stressed that the two determinations for the velocities were performed independently and *not* adjusted to give the best possible fit.

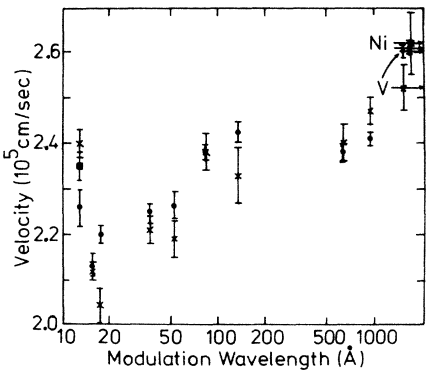

FIG. 4. Phonon velocities obtained from Brillouin scattering (crosses) and SAW (dots) measurements. The square is a control sample which was measured using Brillouin scattering after the SAW measurement.

VI. CONCLUSIONS

The results confirm the lattice softening observed earlier using Brillouin scattering and show that the earlier observations are not due to some peculiarity of light scattering. Moreover, the procedure described in Sec. IV provides a simple and reliable method for the analysis of SAW measurements of thin films.

Returning to the elastic properties of metallic superlattices, it is clear that the softening observed in bcc/fcc superlattices (Ni/Mo, Nb/Cu, and V/Ni) whose constituents do not form solid solutions in their binary phase diagram is a general phenomenon. It has been shown earlier that this softening is correlated with a perpendicular lattice expansion,[7] and a numerical calculation[9] has shown that this lattice expansion is responsible for the softening.

On the other hand, the large enhancement[2,3] claimed in the Young and biaxial and torsional modulii of systems that form solid solutions (Cu/Ni, for instance) have been ascribed to some form of electronic effect.[23] To date, no theory based on the electronic structure has been advanced that can quantitatively explain these enhancements.[6] Since all mechanical measurements leading to enhancements have been performed by removing the sample from the substrates, it would be of considerable interest to perform SAW measurements on "solid-solution" superlattices. Earlier attempts to perform Brillouin scattering measurements in Cu/Ni have been unsuccessful due to the quality of the surface.

ACKNOWLEDGMENTS

We would like to acknowledge useful conversations with M. Levy, C. Falco, and A. Rahman. This work was supported by the U.S. Department of Energy, and by the U.S. Office of Naval Research Contract N00014-83-F-0031.

[1]For a review, see, for instance, I. K. Schuller and C. M. Falco, in *Microstructure Science and Engineering/VLSI,* edited by N. G. Einspruch (Academic, New York, 1982).
[2]W. M. C. Yang, T. Tsakalakos, and J. E. Hilliard, J. Appl. Phys. **48**, 876 (1977); and T. Tsakalakos, Ph.D. thesis, Northwestern University, 1977.
[3]L. R. Testardi, R. H. Willens, J. T. Krause, D. B. McWhan, and S. Nakahara, J. Appl. Phys. **52**, 510 (1980).
[4]B. S. Berry and W. C. Pritchett, Thin Solid Films **33**, 19 (1976).
[5]Hideo Itozaki, Ph.D. thesis, Northwestern University, 1982.
[6]W. E. Pickett, J. Phys. F **12**, 2195 (1982).
[7]A. Kueny, M. Grimsditch, K. Miyano, I. Banerjee, C. Falco, and I. K. Schuller, Phys. Rev. Lett. **48**, 166 (1982).
[8]M. R. Khan, C. S. L. Chun, G. Felcher, M. Grimsditch, A. Kueny, C. M. Falco, and I. K. Schuller, Phys. Rev. B **27**, 7186 (1983).
[9]I. K. Schuller and A. Rahman, Phys. Rev. Lett. **50**, 1377 (1983).
[10]I. K. Schuller and C. M. Falco, in *Inhomogeneous Superconductors-1979 (Berkeley Springs, WV),* Proceeding of the Conference, edited by D. U. Gubser, T. L. Francavilla, J. R. Leibowitz, and S. A. Wolf (AIP, New York, 1979), p. 197.
[11]I. K. Schuller, Phys. Rev. Lett. **44**, 1597 (1980).
[12]H. Homma and I. K. Schuller (unpublished).
[13]H. Homma, C. S. L. Chun, G.-G. Zheng, and I. K. Schuller, Phys. Rev. B (to be published).
[14]C. P. Papadakis, in *Physical Acoustics* edited by W. P. Mason and R. N. Thurston (Academic, New York, 1976), Vol. XII, p. 277.
[15]A. A. Oliner, *Acoustic Surface Waves* (Springer-Verlag, Berlin, 1978).
[16]G. W. Farnell and E. L. Adler, in *Physical Acoustics,* edited by W. P. Mason (Academic, New York, 1973), Vol. IX, p. 35.
[17]H. F. Tiersten, J. Appl. Phys. **40**, 770 (1969).
[18]L. R. Adkins and A. J. Hughes, IEEE Trans. Microwave Theory Tech. **MIT-17**, 904 (1969).
[19]F. Pizzarello, J. Appl. Phys. **43**, 3627 (1972).
[20]D. C. Wolkerstorfer, Ph.D. thesis, Stanford University, 1971.
[21]H. Skeie, J. Acoust. Soc. Am. **48**, 1098 (1970).
[22]R. Haug, Ph.D. thesis, University of Tübingen, 1984.
[23]G. E. Henein, Ph.D. thesis, Northwestern University, 1979.

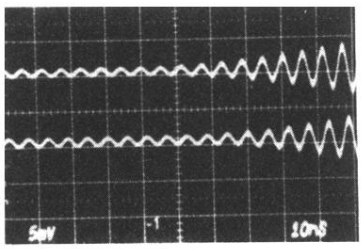

(a)

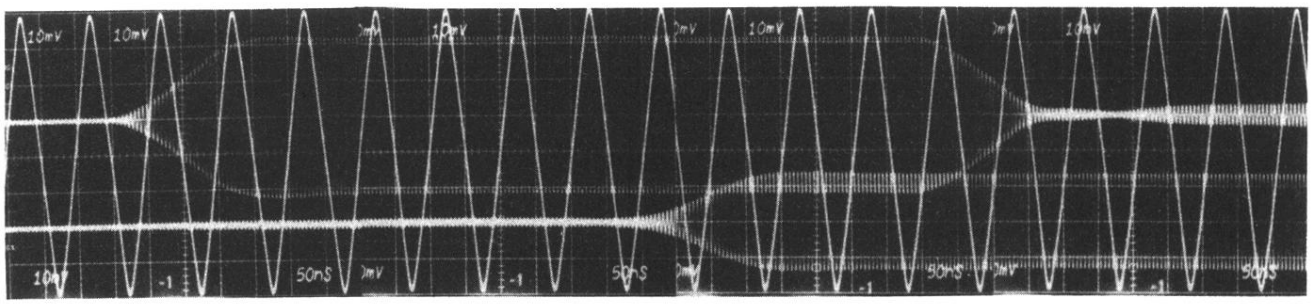

(b)

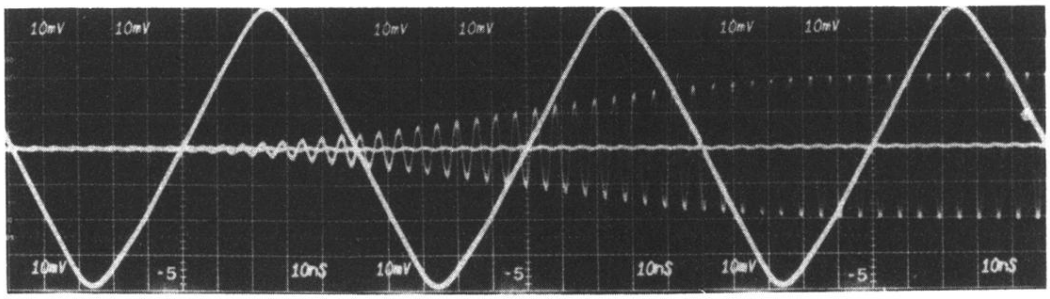

(c)

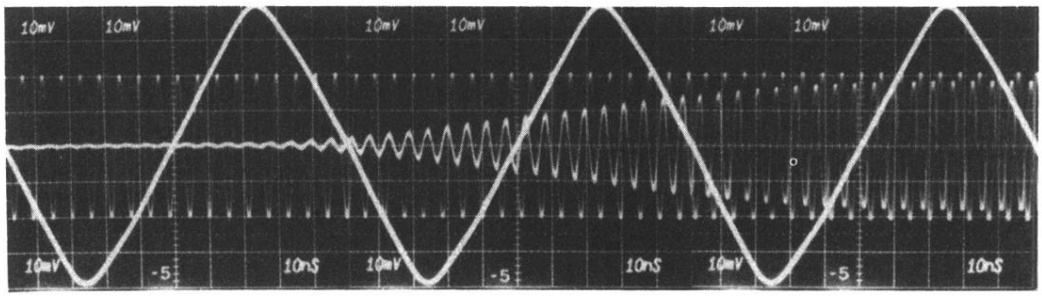

FIG. 3. Oscilloscope traces obtained as described in the text.